

Modeling The Rf Acoustic Behavior Of Love-wave Sensors Loaded With Organic Layers

L. El Fissi, J.-M. Friedt
SENSeOR
399, Route des Crêtes, B.P. 232
06904 Sophia Antipolis Cedex
jean-michel.friedt@senseor.com

S. Ballandras
FEMTO-ST, UMR 6174 CNRS,
32 Ave de l'Observatoire, F-25044 Besançon
sylvain.ballandras@femto-st.fr

Abstract— In order to exploit complicated combinations of measurements associated with acoustic devices, we present the results of finite element/boundary element analyses including visco-elastic losses on fluid-loaded Love-wave based devices, used as microbalance for biochemical detection and sensing purposes. The P-matrix characteristics of the mode are extracted from these computations to simulate the implemented devices. The corresponding frequency dependent phase shift and acoustic losses are introduced in the P-matrix model, allowing for an accurate prediction of insertion losses and phase sensitivity of our Love-wave delay lines. Comparison between theory and experiments shows that we are capable to accurately predict the influence of viscosity on the insertion losses of the Love-wave microbalance.

Index terms – *Sensors, Love wave, viscosity, system simulation, FEM-BEM, P-matrix.*

I. INTRODUCTION

Love mode acoustic wave sensors have demonstrated high detection sensitivity for analytes in liquid media [1]. Beyond the qualitative identification of an analyte, the quantitative interpretation of the physical properties is a complex problem associated to the multitude of possible causes yielding changes in acoustic velocities and insertion losses. Among such phenomena are the adsorbed mass, layer permittivity, viscoelastic properties and temperature. These combined properties yield complex analysis but also provide unique opportunities for identifying such properties in thin organic films.

In order to exploit at best the rich combination of measurements associated with acoustic devices, we present the results of Finite Element Analysis (FEA) models combined with Boundary Element Methods (BEM) developed to simulate the influence of liquid loads and/or visco-elastic losses in adsorbed protein thin films in the reaction area of our Love-wave-based microbalances. Our FEA/BEM simulation tool then has been adapted to account for acoustic radiation into Newtonian viscous fluids [2], allowing for reliable descriptions of actual transducer shapes and operation. For instance, we are able to deduce from these models mass and

viscosity properties of the layer, from which we can extract meaningful quantities for further biosensor modeling including solvent content in the layer, optical index and density.

The P-matrix characteristics of the Love-wave transducers are extracted from these computations to simulate the implemented devices. They consist in delay lines with interdigital transducers protected from the presence of water which would otherwise prevent their normal operation, and a probing area on which are deposited either the probed medium or reactive layers for identification purpose. The corresponding frequency dependent phase shift and acoustic losses are introduced in the P-matrix model, allowing for an accurate prediction of insertion losses and phase sensitivity of our Love-wave delay lines.

Delay-lines operating near 125 MHz have been built exploiting either epoxy-based (SU-8 photo-resist) or silica guiding layers, with typical insertion losses (IL) ranging between 23 and 26 dB. Experimental and theoretical IL-increases of about 3 dB are obtained with water loading the delay line, emphasizing the quality of the simulation approach. The contribution of combinations of glycerol and water loading to the insertion losses is predicted and measured for a 70 wavelength long acoustic probing area. The very good agreement between theory and experiments allows for optimization procedures to be developed, based on this work.

II. DESCRIPTION OF THE LOVE-WAVE-BASED MICROBALANCE

Our Love-wave devices consists in delay lines built on (AT,Z) cut of quartz. The wave guidance is achieved by depositing either a 2.5 μm thick silica overlay or a 1 μm thick epoxy-based (SU-8) layer atop AT-cut of quartz. The Love wave is excited and detected using IDTS composed of 50 pair of 4-finger-per-wavelength electrodes made of 200 nm thick evaporated Aluminium. The grating period is 10 μm , i.e. a wavelength close to 40 μm yielding a frequency operation in the vicinity of 125 MHz. A 3.2 mm long cavity is achieved in between two IDTs, consisting in the location where biochemical reaction are assumed to take place. The acoustic aperture 3.5 mm wide. The acoustic aperture is 3.5 mm. The SU-8 photoresist or the silica overlays used here as guiding layer are patterned

for opening the bonding pads Figure 1 shows a scheme of the delay line and fig.2 shows a photo of the dual line delay line equipped with some fluidics parts directly micromachined atop the devices [3]. One delay line is dedicated to the sensing operation, whereas the other is used as phase and magnitude reference.



Figure1. Scheme of the Love-wave based delay line

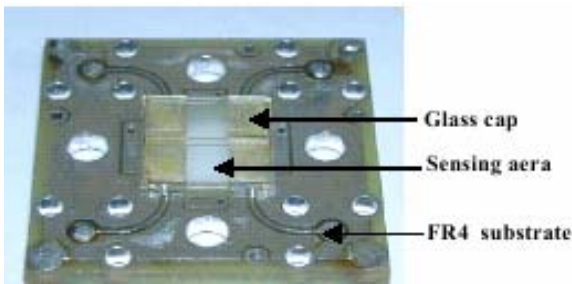
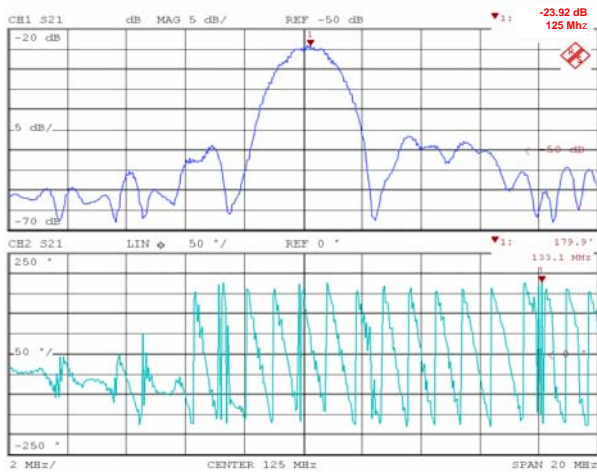
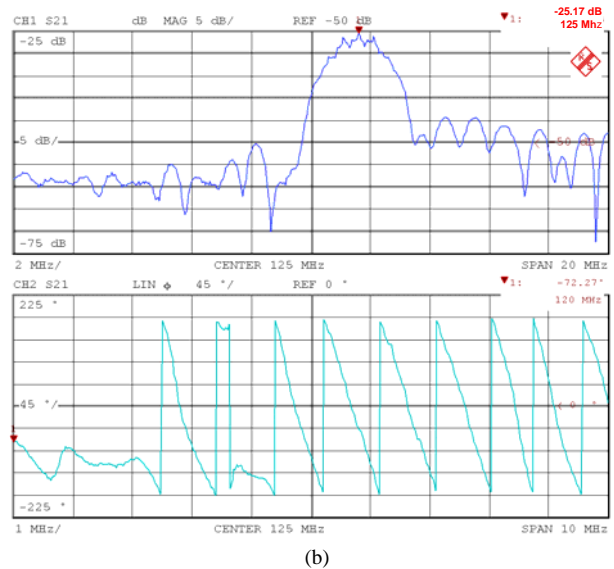


Figure2. Photo of the dual delay line sensor nequiped with microfluidics parts atop the device surface

The delay lines are fabricated using lift-off techniques with appropriate photo-resist to define the IDTs and Aluminium evaporation. Figure 3 a&b show the typical responses of Silica and SU-8 based Love-wave delay lines, showing the possibility to achieve insertion losses (IL) within the delay line pass band in the range 23-25 dB. SU-8 layers are particularly interesting for the possibility they offer to generate selectively sensitive surfaces allowing for specific molecule detection [1, 3]. Absorbing materials have been deposited at the edge of the device to regularize the shape of the transfer function.



(a)



(b)

Figure3. Transfer function of delay line exploiting Silica (a) or SU-8 (b) guiding overlays.

III. DELAY LINE MODELLING

We define here three major steps in the modelling of our devices. In this section, we first show how to account for the excitation and detection of the Love wave, considering the actual shape of the transducer. We then briefly present the evaluation of wave propagation parameters in the sensing area. Finally, we show how to integrate these approaches in a mixed matrix model to simulate the actual operation of the delay line.

A. Transducer modeling

The transducer consists in pairs of splitted finger to favour their operation far from the Bragg condition. This celebrated four-finger-per-wavelength structure is however passivated by the guiding layer, which does not ease the simulation of its acousto-electric operation. We then use our periodic FEA-BEM simulation tool to account for the actual shape of one mechanical period of the IDT. In that matter, we actually consider that the overlay conforms the initial shape of the transducer, yielding the mesh of fig.4. To simply simulate the working of the transducer, we apply a phase condition corresponding to an harmonic excitation in quadrature, allowing for simply representing the actual voltage conditions applid to the transducer.

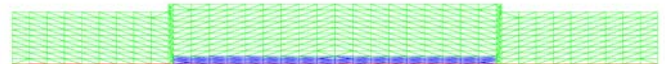


Figure4. Mesh of one elementary electrode (one mechanical period) of a 4-finger-per-wavelength IDT. The overlay is assumed conformal, i.e. it reproduces the initial shape of the transducer on the top surface. The green part corresponds to the guiding layer, the blue to the electrode, the interface between FEA and BEM is symbolized by the red line [4]

As we are far from the Bragg condition, we don't have to care about any kind of stop-band effect and we simply analyse the pole on the harmonic admittance which give us all the information we are looking for, i.e. the phase velocity, the coupling strength and the acoustic losses, mainly due to the fact that the implemented guiding layers generally exhibit non negligible visco-elastic effects. According to Fusero [5], we consider the following formulas to extract those parameters :

$$V = f_{res} \cdot \lambda, \quad G = p\pi \frac{f_B - f_H}{f_B + f_H} (Y(f_B) + Y(f_H)) \quad (1)$$

$$\chi = 40 \log e\pi \frac{f_B - f_H}{f_B + f_H}$$

where V is the phase velocity, G the conductance and χ the loss coefficient. The definition of frequencies f_B and f_H appears in fig.5

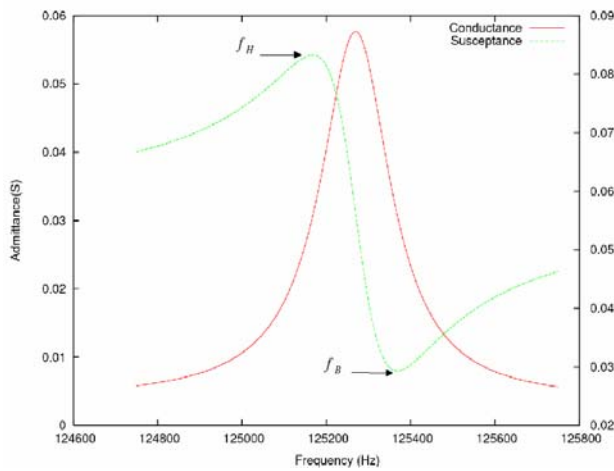


Figure5. Pseudo-pole of the harmonic admittance for a phase quadrature excitation applied to the mesh of fig.4

B. Propagation parameters

The simulation of acoustic propagation parameters is much simpler than the one of the transduction area of the device, since plane interfaces allows for developing analytic harmonic models allowing for the derivation of surface or interface Green's functions [2] from which the phase velocity and loss coefficient can be easily deduced. The model is presented in detail in ref [2]. We then only reproduc here the results when have obtained by considering different concentrations of glycerol/water compound atop the silica-based Love wave guide. The evolution of the acoustic velocity and losses versus Glycerol concentration is plotted in fig.6. It shows that the wave velocity is significantly affected by the viscosity of the liquid. This must be accounted for when measuring adsorbed molecules atop the sensing area, to correctly separate the different involved effects, i.e. mass loading and viscosity changes. In the present case, we nevertheless have to account for the role of the transducer which is not submitted to the

water load, and which contributes in a non negligible matter to the actual central frequency location of the delay line.

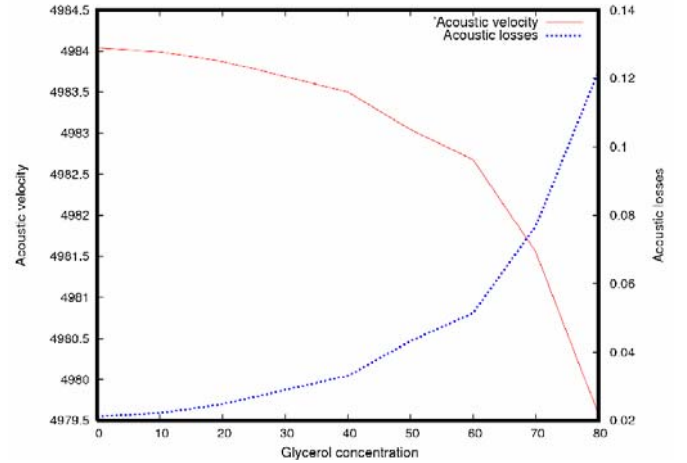


Figure6. Phase velocity and acoustic losses versus glycerol concentration (velocity in $m.s^{-1}$, losses in dB/λ)

C. Mixed matrix model of the transducer

The final theoretical development of this work deals with the simulation of the whole device, i.e. the combination of IDT and sensing area contributions to the final transfer function of the device. As explained above, we extract coupling and propagation parameters from the FEA-BEM model. Since no reflection occurs in the IDT, the mixed matrix model of one cell can be represented as follows :

$$\begin{Bmatrix} S_1 \\ S_2 \\ I \end{Bmatrix} = \begin{bmatrix} 0 & e^{-j\varphi} & \alpha_1 \\ e^{+j\varphi} & 0 & \alpha_2 \\ -\alpha_1 & -\alpha_2 & G + jB \end{bmatrix} \begin{Bmatrix} E_1 \\ E_2 \\ V \end{Bmatrix} \quad (2)$$

where G and B are respectively the linked conductance and susceptance of the cell, α represent the electromechanical coupling and φ the propagation phase, accounting for acoustic losses. In a very similar way, the propagation surface is simply represented by the following transfer matrix

$$\begin{Bmatrix} S_1 \\ S_2 \end{Bmatrix} = \begin{bmatrix} 0 & e^{-j\varphi} \\ e^{+j\varphi} & 0 \end{bmatrix} \begin{Bmatrix} E_1 \\ E_2 \end{Bmatrix} \quad (2)$$

Both section of the model are coupled together in a usual matrix cascade, providing the simulation results we are looking for.

IV. EXPERIMENTAL ASSESSMENT

These developments have to be confirmed and validated by experiments. We then loaded the sensing area of our Love-wave delay lines with water/glycerol compounds,

progressively increasing the glycerol concentration and monitoring the corresponding insertion losses of the device. We then have superimposed the predicted insertion losses to the measured ones, allowing to prove the accuracy of our prediction on an extended range of equivalent viscosity (1-20 cP). Figure 7 shows the comparison between experimental and theoretical results. One can note that for high glycerol concentrations, the stabilisation of the insertion losses is far to be immediate, and relaxation phenomena not accounted in our model seem to occur. Due to the nature of such behaviour, the proposed linear model cannot address that problem, which will require more developments to reach such a goal. We also report the evolution of the delay line central frequency, for which some work still has to be achieved for a convincing comparison between theory and experiments.

V. CONCLUSION

The simulation of Love-wave delay lines used as sensors for the characterization of in-liquids molecule concentrations and fluid properties has been proposed and implemented in this work. Specific sections of the delay lines have been treated separately, and merged into a mixed matrix model allowing for the global simulation of the sensor. An experimental set-up also has been implemented, operating near 125 MHz, to assess the model quality. The very good agreement between theoretically predicted insertion losses and actual measurements have proven the accuracy of the model. Some work still has to be achieved to confirm the capability of the model to predict the evolution of the central frequency too. Also the model limits have been somehow identify, missing the possibility to predict relaxation phenomena that seem to occur for 70% glycerol concentration, since the model is based on linear equations. More advanced developments will be necessary to account for such phenomena, and will consist in one of our future developments. However, we already have access to an accurate model allowing for a more realistic optimisation of the sensing systems integrating Love-wave-based microbalances.

REFERENCES

The authors would like to thank Thomas Pastureaud for his mixed matrix developments, as well as Raphaël Lardat for his help in developing the FEA-BEM code, and finally Gerhard Heider (SENSeOR's CEO) for his help in the work promotion.

REFERENCES

1] L. Francis, J.-M. Friedt, C. Bartic, A. Campitelli, A SU8 liquid cell for surface acoustic waves biosensors, SPIE proceedings series 5455, pp. 353-363 (2004)

2] S. Ballandras, A. Reinhardt, A. Khelif, M. Wilm, V. Laude, W. Daniau, V. Blondeau-Pâtissier, "Theoretical analysis of damping effects of guided elastic waves at solid/fluid interfaces", Journal of Applied Physics. 2006.99.054907
 3] L.El Fissi, J.M. Friedt, F. Chérioux, V. Blondeau-Pâtissier, S. Ballandras, Design and use of wafer level fluidic packaging for surface acoustic wave sensors, Proc. of the IEEE International Frequency Control Symposium, Geneva, 2007
 4] Y. Fusero, S. Ballandras, J. Desbois, J.M. Hodé, P. Ventura, "SSBW-to-PSAW conversion in SAW devices using heavy mechanical loading", IEEE Trans. on UFFC, Vol. 49, n°6, pp. 805-814, 2002
 5] S. Ballandras, V. Laude, A. Reinhardt, M. Wilm, R. Lardat, W. Steichen, T. Pastureaud, "Optimisation and Improved Convergence of Coupled Finite Element/Boundary Element Analyses?", proc. of the IEEE Ultrasonics Symp., pp. 679- 682, 2005

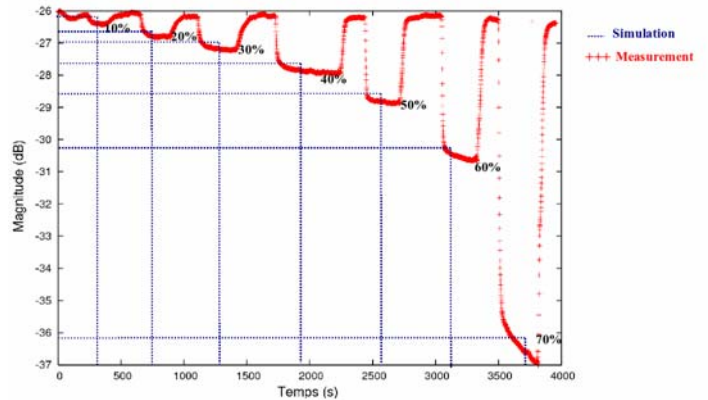
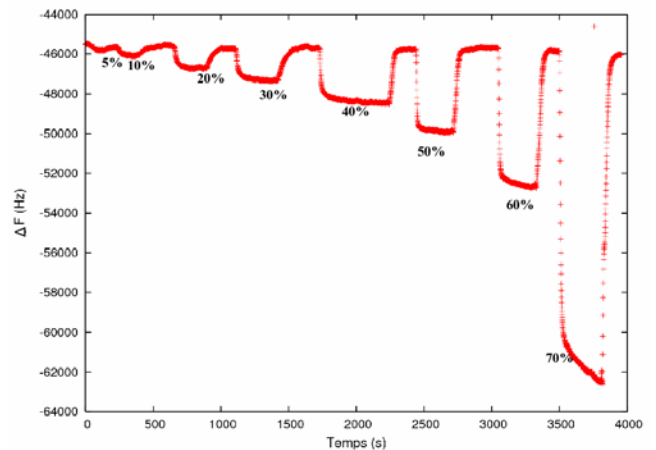


Figure7. Evolution of experimental insertion losses monitored for different concentration of glycerol, superimposition of predicted insertion loss values



concentration. The variations are smaller than the one predicted by only considering the sensing area behaviour. The role of the IDTs in that matter has to be identified.